

Adiabatic passage of light in coupled optical waveguides

Stefano Longhi

*Dipartimento di Fisica and Istituto di Fotonica e Nanotecnologie del CNR, Politecnico di Milano,
Piazza L. da Vinci 32, I-20133 Milan, Italy*

(Received 26 September 2005; published 13 February 2006)

Adiabatic passage of light in coupled optical waveguides with a curved axis is theoretically investigated and shown to bear a close connection with coherent population transfer among quantum states of atoms and molecules. In particular, the optical analog of stimulated Raman adiabatic passage can be realized in a three-waveguide optical directional coupler.

DOI: 10.1103/PhysRevE.73.026607

PACS number(s): 32.80.Qk, 42.82.Et, 82.53.Kp

INTRODUCTION

Owing to the strong similarity between quantum mechanics and wave optics, light propagation in photonic structures has provided on many occasions a useful and easily accessible laboratory tool to investigate several coherent quantum effects that may be more difficult to observe or investigate in atomic, molecular, or condensed-matter systems due to, e.g., unavoidable dephasing effects or fast temporal dynamics. Examples of optical realizations of coherent quantum effects include optical Bloch oscillations [1–3] and optical dynamic localization [4,5] in arrayed waveguides, adiabatic stabilization, and wave packet dichotomy of light in periodically curved waveguides [6,7], quantum tunneling enhancement and suppression in optical directional couplers [8,9], and Landau-Zener dynamics in coupled waveguides [10]. An important phenomenon of coherent temporal evolution encountered in quantum systems is that of coherent population transfer among discrete states of atoms or molecules by use of partially overlapped optical laser pulses, which has found many applications in molecular dynamics and spectroscopy, chemical reaction dynamics, quantum optics, and atom optics (for a recent review on this subject see, e.g., [11] and references therein). The simplest case is that of a three-state system and stimulated Raman adiabatic passage (STIRAP), which is a remarkable example of counterintuitive physics [11–13]. In the STIRAP a Stokes pulse, driving the transition between the initially unpopulated levels 2 and 3, coherently prepares the system and precedes a partially overlapped pump pulse, which drives the transition between the initially populated level 1 and the intermediate level 2. Population transfer from level 1 to level 3 is achieved by adiabatic passage of an instantaneous dressed state, the population placed in the intermediate state 2 during the adiabatic transfer being small or even negligible. The main interest on the STIRAP stems from its capability of providing excitation between states of the same parity, for which electric dipole transitions are forbidden, by an intermediate state; in addition the counterintuitive scheme, where the Stokes pulse precedes the pump pulse, does not populate the intermediate level, and it is therefore insensitive to any possible decay of the intermediate state.

In this paper an optical realization of coherent adiabatic passage of light is theoretically proposed using coupled waveguides with a bent axis, in which light propagation

along different waveguides exactly mimics the coherent temporal population dynamics of the STIRAP.

THE MODEL

The starting point of the analysis is provided by a standard model of beam propagation at wavelength $\lambda=2\pi/k$ in an optical coupler, made of a chain of N waveguides written along the Z direction and lying in the (X,Z) plane [Fig. 1(a)]. The waveguides are assumed to be single mode and of different design [Fig. 1(b)] so that the propagation constants of the fundamental waveguide modes of the various waveguides are not degenerate. The axis of the waveguides is assumed to be straight in the first and last sections of the waveguides, with an intermediate section in which the axis is bent along the propagation direction Z with a bending profile $X_0(Z)$ which is assumed to vary slowly over a distance of the order of λ . Typically, we assume that the bending profile is a biharmonic (or polyharmonic) function with a smooth envelope that goes to zero connecting the initial and final straight waveguide sections [Fig. 1(a)]. Without loss of generality, we further assume that the field is strongly localized in the vertical Y direction by a planar waveguiding structure, so that beam dynamics can be effectively reduced to a two-dimensional problem [14]. For a weak refractive index change of the waveguide channels from the substrate

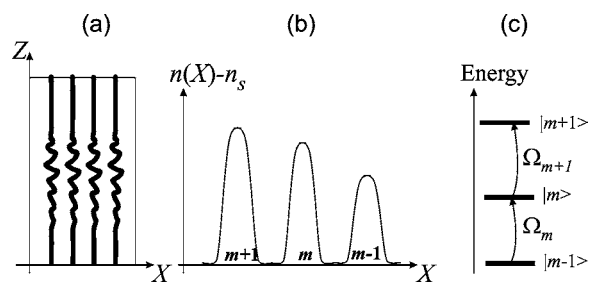


FIG. 1. (a) The schematic of a waveguide coupler made of a chain of waveguides with a bent axis. (b) The refractive index profile $n(x)-n_s$ of the coupler with three waveguides m , $m+1$, and $m+2$. (c) The quantum-mechanical equivalence between bending-induced waveguide coupling and coherent population transfer. The transfer between $|m-1\rangle$, $|m\rangle$, and $|m+1\rangle$ states is induced by axis bending harmonic components Ω_m [see Eq. (7) in the text].

refractive index n_s , the electric field can be written as $E(X, Z, t) = \psi(X, Z) \exp(ikn_s Z - i\omega t) + \text{c. c.}$, where $\omega = kc_0$ and the envelope $\psi(X, Z)$ satisfies the scalar and paraxial wave equation (see, e.g., [6,9,15])

$$i\lambda \frac{\partial \psi}{\partial Z} = -\frac{\lambda^2}{2n_s} \frac{\partial^2 \psi}{\partial X^2} + V(X - X_0(Z))\psi, \quad (1)$$

where $\lambda \equiv \lambda/(2\pi)$, $V(X) \equiv [n_s^2 - n^2(X)]/(2n_s) \approx n_s - n(X)$, and $n(X)$ is the refractive index profile of the coupler when the waveguides are straight [Fig. 1(b)]. It was previously shown [6] that, after the Kramers-Henneberger transformation $x = X - X_0(Z)$, $z = Z$, $\phi(x, z) = \psi(x, z) \exp[-i\lambda \dot{X}_0 x/n_s - i(n_s/2\lambda) \int_0^z d\xi \dot{X}_0^2(\xi)]$, where the dot indicates the derivative with respect to z , Eq. (1) yields the following wave equation for the envelope $\phi(x, z)$

$$i\lambda \frac{\partial \phi}{\partial z} = -\frac{\lambda^2}{2n_s} \frac{\partial^2 \phi}{\partial x^2} + V(x)\phi - q\mathcal{E}(z)x\phi, \quad (2)$$

where we have set

$$q\mathcal{E}(z) \equiv -n_s \ddot{X}_0(z). \quad (3)$$

After the formal substitution $z \rightarrow t$, $n_s \rightarrow m$, and $\lambda \rightarrow h$, Eq. (2) describes the semiclassical quantum dynamics, in the electric dipole approximation, of a particle of mass m and charge q in the potential $V(x)$ subjected to an external electric field $\mathcal{E}(z)$, which is related to the waveguide axis bending through Eq. (3). Note that the field $\mathcal{E}(z)$ is polychromatic with the same harmonic content of the bending profile $X_0(z)$.

COUPLED MODE EQUATIONS

In order to highlight the close connection between beam dynamics along the curved optical coupler and coherent population transfer in quantum systems, it is worth deriving a set of coupled mode equations for the amplitudes of waveguide modes [16]. To this aim, let us indicate by $\mathcal{H}_0 \equiv -\lambda^2/(2n_s) \partial_x^2 + V(x)$ the Hamiltonian operator of Eq. (2) in absence of bending, and by $w_n(x)$ and $\lambda\omega_n$ the eigenfunctions (also called supermodes of the structure [16]) and corresponding eigenvalues of \mathcal{H}_0 , with the normalization condition $\langle w_n | w_m \rangle = \delta_{nm}$. As discussed in the Appendix, in the case where the waveguides are weakly coupled and their individual fundamental modes are not degenerate, the supermodes $w_n(x)$ and corresponding eigenvalues $\lambda\omega_n$ are close to the eigenmodes $u_n(x)$ and corresponding propagation constants β_n of the single n th waveguide of the chain. To study the effect of waveguide axis bending perturbation $\mathcal{H}' = -q\mathcal{E}(z)x$ on mode dynamics, we assume that bending-induced coupling into radiation modes is small, so that the envelope $\phi(x, z)$ can be expanded as a superposition of supermodes $w_n(x)$ with coefficients that depend on z , namely

$$\phi(x, z) = \sum_n a_n(z) w_n(x) \exp(-i\omega_n z). \quad (4)$$

The evolution equations for the amplitudes $a_n(z)$ induced by the perturbation \mathcal{H}' can be derived from Eq. (2) by a stan-

dard mode projection technique and read explicitly

$$i\lambda \dot{a}_n = -\sum_m a_m(z) \mu_{n,m} q\mathcal{E}(z) \exp[i(\omega_n - \omega_m)z], \quad (5)$$

where the dot denotes the derivative with respect to z and where we have set

$$\mu_{n,m} \equiv \langle w_n | x | w_m \rangle = \int dx w_n^*(x) x w_m(x). \quad (6)$$

Note that, since the supermode frequencies ω_n are not degenerate, for small values of the force $q\mathcal{E}$ (a condition required to avoid large bending-induced radiation losses), we can neglect in Eq. (5) the rapidly varying terms (rotating-wave approximation); in addition, since the coefficients $\mu_{n,m}$ rapidly decay to zero as $|m-n|$ increases due to mode displacement, we may assume $\mu_{n,m} \sim 0$ for $|n-m| > 1$ (nearest-neighbor approximation). Under such conditions, Eq. (5) take the simplified form [17]

$$i\dot{a}_n = \frac{1}{2}(\Omega_n^* a_{n-1} + \Omega_{n+1} a_{n+1}), \quad (7)$$

where $\Omega_n = -(2\mu_{n-1,n}/\lambda) q\mathcal{E}(z) \exp[-i(\omega_n - \omega_{n-1})z]$ and the overline denotes a spatial average. The form of such equations is analogous to the Hamiltonian equations of the STIRAP processes in multilevel quantum systems involving coherent multiphoton excitation [11], Ω_n playing the role of the Rabi frequencies of the near-resonant exciting fields [Fig. 1(c)].

ADIABATIC LIGHT PASSAGE

The simplest case of adiabatic light passage, which provides the optical analog of the STIRAP in a three level quantum system [Fig. 1(c)], is that of three waveguides with a biharmonic bending axis profile of the form

$$X_0(z) = A_p(z) \cos[(\omega_2 - \omega_1)z] + A_s(z) \cos[(\omega_3 - \omega_2)z], \quad (8)$$

where the slowly varying envelopes A_p and A_s simulate the pulse shapes of pump and Stokes fields. In this case, Eq. (7) read explicitly

$$i \frac{d}{dt} \begin{pmatrix} a_1 \\ a_2 \\ a_3 \end{pmatrix} = \frac{1}{2} \begin{pmatrix} 0 & \Omega_p & 0 \\ \Omega_p^* & 0 & \Omega_s \\ 0 & \Omega_s^* & 0 \end{pmatrix} \begin{pmatrix} a_1 \\ a_2 \\ a_3 \end{pmatrix},$$

where $\Omega_p(z) \approx -[n_s \mu_{12} A_p(z)]/[\lambda(\omega_2 - \omega_1)^2]$ and $\Omega_s(z) \approx -[n_s \mu_{23} A_s(z)]/[\lambda(\omega_3 - \omega_2)^2]$. The dynamics of the STIRAP, which has been extensively studied in many works (we refer the reader to [11] and references quoted therein), requires the Stokes pulse Ω_s to precede the pump pulse Ω_p , allowing in the adiabatic limit an almost complete transition of the system from the initial state $\mathbf{a} = (1, 0, 0)$, corresponding in the optical system to initial excitation of the waveguide 1, into the final state $\mathbf{a} = (0, 0, 1)$, corresponding to the light coming out from waveguide 3, with small excitation of the intermediate waveguide 2. Such a dynamical behavior is based upon adiabatic following of an instantaneous dressed state that passes continuously from state $\mathbf{a} = (1, 0, 0)$ to state $\mathbf{a} = (0, 0, 1)$ [11]. In the adiabatic limit, the dynamics is not

appreciably influenced by the specific shapes of pump and Stokes pulses.

The optical realization of the STIRAP provides an interesting and counterintuitive technique to couple light from waveguide 1 into waveguide 3 through an intermediate waveguide 2, which is however weakly excited during the light transfer process. Such a light transfer mechanism may be referred to as adiabatic light passage in analogy to the equivalent quantum mechanical process in three-state systems.

NUMERICAL RESULTS

We checked the occurrence of adiabatic light passage and the STIRAP in a three-waveguide coupler with a biharmonic bending axis profile by a direct numerical integration of the scalar wave equation (1) using a pseudospectral split-step beam propagation technique, and compared the numerical results with those predicted by the coupled-mode equation analysis. Equation (1) has been solved on a domain with a finite extension in the transverse x direction and assuming absorbing boundary conditions to account for bending-induced radiation losses (for details see [6]). The refractive index profile of each waveguide forming the coupler has been assumed to be of the form [18] $n(x) = n_s + \Delta n \{ \text{erf}[(x+w)/D_x] - \text{erf}[(x-w)/D_x] \} / [2 \text{erf}(w/D_x)]$, where $2w$ and D_x are the channel width and the lateral diffusion length, respectively. The separation between adjacent waveguides is a . The nondegeneracy of waveguide modes is obtained by assuming different values for the index change Δn [19]. Parameter values have been chosen for typical lithium-niobate waveguides excited at $\lambda = 1.5 \mu\text{m}$. The index profile of the coupler used in our numerical simulations is shown in Fig. 2(a), whereas Fig. 2(b) depicts the profiles of the three supermodes $w_n(x)$ of the waveguide chain, calculated by a direct numerical computation of eigenmodes and eigenvalues of \mathcal{H}_0 , together with the mode profiles of the individual waveguide. Note that, as expected from the variational analysis presented in the Appendix, the profiles of the supermodes are well approximated by the fundamental modes of each individual waveguide of the chain. Figure 2(c) shows the biharmonic bending profile of the waveguide axis, which is obtained by assuming a Gaussian shape $A_p(z) = A_{p0} \exp[-(z-L/2+z_0)^2/\Lambda^2]$ and $A_s(z) = A_{s0} \exp[-(z-L/2-z_0)^2/\Lambda^2]$ for the slowly-varying pump and Stokes field envelopes, where L is the total waveguide length, z_0 determines the overlap fraction of the two fields, and 2Λ is the width of the two envelopes.

The spatial periods of the two harmonics forming the biharmonic bending profile turn out to be $2\pi/|\omega_2 - \omega_1| \sim 800 \mu\text{m}$ and $2\pi/|\omega_3 - \omega_2| \sim 310 \mu\text{m}$ for the pump and Stokes fields, respectively. Note that the maximum excursion of transverse axis displacement from straightness has been chosen less than the waveguide width $2w$ in order to keep radiation losses at a small level. Figure 3 shows a gray-scale plot of beam propagation along the coupler, in the (x, z) plane, as obtained when the waveguide on the right hand side (guide number 1) is initially excited in its fundamental mode, together with the input and output intensity beam profiles [Fig. 3(b)] and total beam power contained in the integration

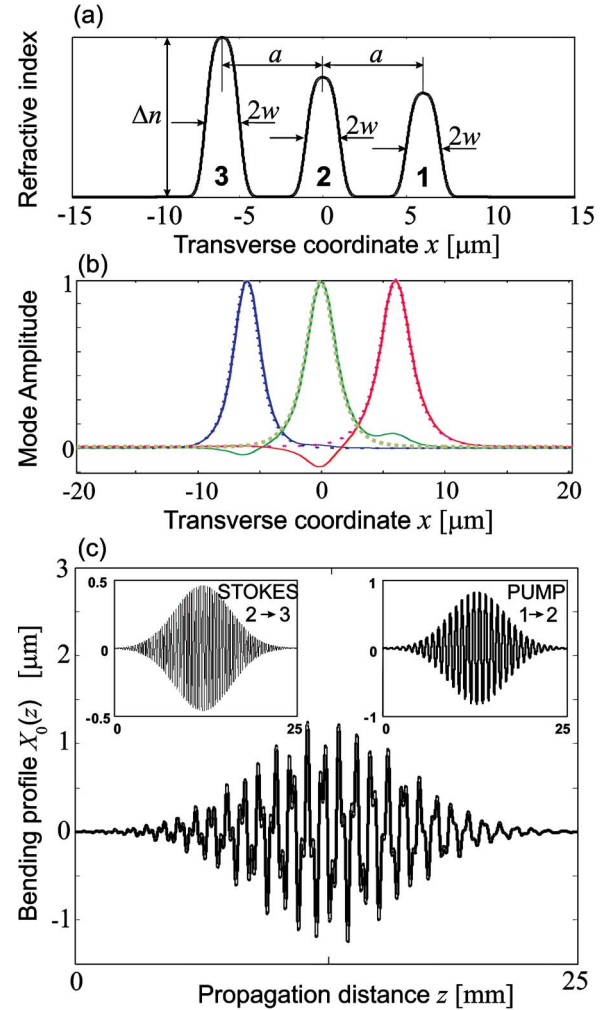


FIG. 2. (Color online) (a) The refractive index profile of a $L=25$ -mm-long three-waveguide coupler used in numerical simulations. The refractive index change for the waveguides are $\Delta n_1=0.0173$, $\Delta n_2=0.02$, and $\Delta n_3=0.0266$. The other parameter values are $n_s=2.14$, $w=1 \mu\text{m}$, $a=6 \mu\text{m}$, and $D_x=0.5 \mu\text{m}^{-1}$. (b) The amplitude profiles of supermodes $w_n(x)$ of the three-waveguide coupler (solid curves) and corresponding profiles of each individual waveguide mode $u_n(x)$ (dotted curves). (c) The biharmonic axis bending profile of the waveguides with Gaussian envelopes for parameter values $A_{s0}=0.46 \mu\text{m}$, $A_{p0}=0.83 \mu\text{m}$, $z_0=360 \mu\text{m}$, and $\Lambda=5380 \mu\text{m}$. The insets show the two harmonic components corresponding to pump and Stokes pulses (the spatial period of the two components are $\sim 800 \mu\text{m}$ and $\sim 310 \mu\text{m}$, respectively).

domain [Fig. 3(c)]. Note that, according to the STIRAP model, a good adiabatic light transfer from waveguide 1 to waveguide 3 is obtained, with small excitation of the intermediate waveguide 2 and with small radiation losses [less than 10%, see Fig. 3(c)]. Figure 4(a) depicts the numerically computed fraction of total beam power carried in the fundamental modes of the three waveguides, showing the adiabatic passage mediated by the intermediate waveguide. Figures 4(b) and 4(c) show the corresponding behavior as obtained by a numerical integration of the coupled-mode equation (5) and the STIRAP equation (7), respectively.

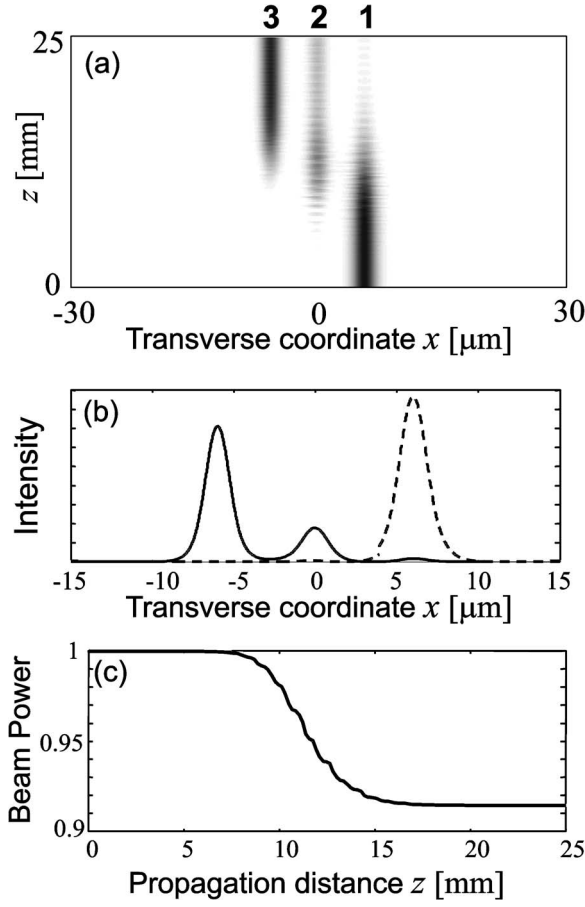


FIG. 3. (a) The gray-scale plot of numerically computed beam evolution along the coupler, showing adiabatic light passage from waveguide 1 to waveguide 3. (b) The intensity beam profiles at the input (dashed curve) and output (solid curve) planes of the coupler. (c) The total beam power $\int |\psi|^2 dx$, normalized to its input value, contained in the transverse $60\text{-}\mu\text{m}$ -wide integration window.

Note that, in the case of Fig. 4(c), the low-amplitude fast oscillations observed in the curves of Figs. 4(a) and 4(b) are absent, which is due to the rotating-wave approximation used in deriving Eq. (7) from Eq. (5). The reasonably good agreement of the curves in Fig. 4(c), obtained from the STIRAP model (7), with those depicted in Figs. 4(a) and 4(b) proves that the basic mechanism underlying light transfer in the coupler is adiabatic passage indeed.

CONCLUSIONS

It has been theoretically shown that the phenomenon of coherent population transfer and the STIRAP in multistate quantum systems can be elegantly realized in curved optical waveguide couplers, with a biharmonic bending profile of the waveguide axis which simulates the effect of pump and Stokes pulses. Adiabatic light passage has been confirmed by a direct numerical integration of the wave equation in a three waveguide coupler. The present analysis provides a remarkable optical analogy of a counterintuitive quantum phenomenon and may stimulate an experimental observation of an optical STIRAP in a waveguide-based system.

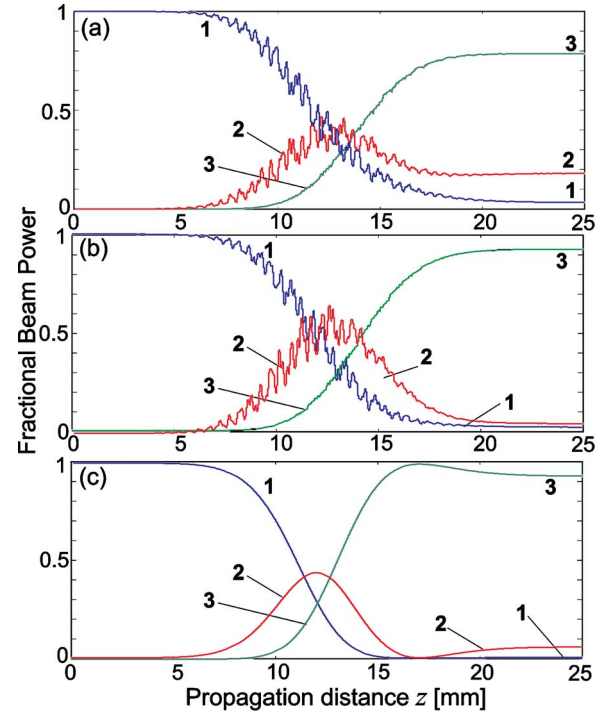


FIG. 4. (Color online) The fractional beam power $|a_m(z)|^2$ versus propagation distance localized in the three waveguides as obtained (a) by numerical simulations of the wave equation, (b) by numerical solutions of the coupled-mode equation (5), and (c) by numerical solutions of the STIRAP equations (7). In (a) the fractional beam power is calculated by mode projection according to $|a_m|^2 = |\int dx u_m^*(x) \phi(x, z)|^2 / |\int dx |\phi(x, z)|^2$.

APPENDIX: SUPERMODES OF A CHAIN OF WAVEGUIDES

For a waveguide structure composed by weakly interacting single-mode and nondegenerate waveguides, the supermodes $w_n(x)$ and corresponding propagation constants λ_{ω_n} of the structure, defined as the eigenmodes and eigenvalues of the Hamiltonian \mathcal{H}_0 , can be perturbatively constructed from the fundamental waveguide modes $u_n(x)$ and propagation constants β_n of individual waveguides using a variational technique. To this aim, let us note that Eq. (2), in absence of the external force ($q\mathcal{E}=0$), can be derived from the variational principle $\delta \int dt dx \mathcal{L} = 0$ with the Lagrangian density

$$\mathcal{L} = \frac{\lambda^2}{2n_s} |\phi_x|^2 + \frac{i\lambda}{2} (\phi \phi_t^* - \phi_t^* \phi) + V(x) |\phi|^2. \quad (\text{A1})$$

Indicating by $u_n(x)$ the fundamental mode of the n th waveguide of the coupler and assuming weak waveguide coupling, we may make the Ansatz $\phi(x, t) = \sum_n c_n(z) u_n(x)$, where the evolution equations for the mode amplitudes $c_n(z)$ are given by the Euler-Lagrange equations $(\partial \mathcal{L}_{red} / \partial c_n) - d/dt (\partial \mathcal{L}_{red} / \partial \dot{c}_n) = 0$ for the reduced Lagrangian $\mathcal{L}_{red} = \int dx \mathcal{L}$.

After some straightforward algebra one obtains the following set of coupled-mode equations:

$$i \chi \dot{\mathbf{c}} = \alpha^{-1} \beta \mathbf{c}, \quad (\text{A2})$$

where \mathbf{c} is the column vector of mode amplitudes c_n , and the z -independent Hermitian matrices α and β are given by

$$\alpha_{n,m} = \int dx u_n^* u_m,$$

$$\beta_{n,m} = \int dx u_n^* \left[-\frac{\chi^2}{2n_s} \frac{d^2 u_m}{dx^2} + V u_m \right]. \quad (\text{A3})$$

If $\phi(x,t)$ is a supermode of the waveguide chain with propagation constant $\chi\omega_m$, one should have $\mathbf{c}(z) = \bar{\mathbf{c}}^{(m)} \exp(-i\chi\omega_m z)$. From Eq. (A2) one then finds [20]

$$\chi\omega_m \bar{\mathbf{c}}^{(m)} = \alpha^{-1} \beta \bar{\mathbf{c}}^{(m)}, \quad (\text{A4})$$

i.e., the amplitudes $\bar{\mathbf{c}}^{(m)}$ are the eigenvectors of the matrix $\alpha^{-1}\beta$ and $\chi\omega_m$ are the corresponding eigenvalues. The supermode profile $w_m(x)$ is then obtained as a superposition of individual waveguide modes $u_n(x)$ according to $w_m(x) = \sum_n \bar{c}_n^{(m)} u_n(x)$. Note that, since we assume that the waveguides are weakly coupled, the matrices α and β are almost diagonal, with $\alpha_{n,n} = 1$ (normalization condition), and $\beta_{n,n}$ almost coincident with the propagation constant β_n of the fundamental mode of the n th waveguide in the chain. Since the propagation constants β_n of the individual waveguides are assumed to be nondegenerate, the matrix $\alpha^{-1}\beta$ has simple eigenvalues, and at leading order $\chi\omega_m \sim \beta_m$, $\bar{c}_n^{(m)} \sim \delta_{m,n}$, and $w_m(x) \sim u_m(x)$.

-
- [1] R. Morandotti, U. Peschel, J. S. Aitchison, H. S. Eisenberg, and Y. Silberberg, *Phys. Rev. Lett.* **83**, 4756 (1999).
- [2] T. Pertsch, P. Dannberg, W. Elflein, A. Bräuer, and F. Lederer, *Phys. Rev. Lett.* **83**, 4752 (1999).
- [3] G. Lenz, I. Talanina, and C. M. de Sterke, *Phys. Rev. Lett.* **83**, 963 (1999).
- [4] G. Lenz, R. Parker, M. C. Wanke, and C. M. de Sterke, *Opt. Commun.* **218**, 87 (2003).
- [5] S. Longhi, *Opt. Lett.* **30**, 2137 (2005).
- [6] S. Longhi, D. Janner, M. Marano, and P. Laporta, *Phys. Rev. E* **67**, 036601 (2003).
- [7] S. Longhi, M. Marangoni, D. Janner, R. Ramponi, P. Laporta, E. Cianci, and V. Foglietti, *Phys. Rev. Lett.* **94**, 073002 (2005).
- [8] I. Vorobeichik, E. Narevicius, G. Rosenblum, M. Orenstein, and N. Moiseyev, *Phys. Rev. Lett.* **90**, 176806 (2003).
- [9] S. Longhi, *Phys. Rev. A* **71**, 065801 (2005).
- [10] R. Khomeriki and S. Ruffo, *Phys. Rev. Lett.* **94**, 113904 (2005).
- [11] K. Bergmann, H. Theuer, and B. W. Shore, *Rev. Mod. Phys.* **70**, 1003 (1998).
- [12] B. W. Shore, *The Theory of Coherent Atomic Excitation* (Wiley, New York, 1990).
- [13] F. T. Hioe and J. H. Eberly, *Phys. Rev. Lett.* **47**, 838 (1981); J. Oreg, F. T. Hioe, and J. H. Eberly, *Phys. Rev. A* **29**, 690 (1984); C. E. Carroll and F. T. Hioe, *J. Opt. Soc. Am. B* **5**, 1335 (1988); J. Oreg, K. Bergmann, B. W. Shore, and S. Rosenwaks, *Phys. Rev. A* **45**, 4888 (1992); N. V. Vitanov and S. Stenholm, *ibid.* **55**, 648 (1997).
- [14] A. A. Sukhorukov, Y. S. Kivshar, H. S. Eisenberg, and Y. Silberberg, *IEEE J. Quantum Electron.* **39**, 31 (2003).
- [15] K. Kawano and T. Kitoh, *Introduction to Optical Waveguide Analysis: Solving Maxwell's Equations and the Schrödinger Equation* (Wiley-Interscience, New York, 2001).
- [16] A. Yariv, *Optical Electronics*, Fourth edition (Saunders College Publishing, New York, 1991), pp. 519–529.
- [17] The bending profile is assumed to have a zero mean value, so that $q\mathcal{E}(z) = 0$. The spatial average has to be taken over a spatial scale of the order of $1/|\omega_n - \omega_{n-1}|$, so that the amplitudes Ω_n may slowly depend on z .
- [18] A. Sharma and P. Bindal, *Opt. Quantum Electron.* **24**, 1359 (1992).
- [19] It should be noted that nondegeneracy of waveguide modes can be achieved as well by assuming different channel widths w and the same refractive index change Δn , a design which is easier for an experimental realization.
- [20] Note that the eigenvalue equation (A4) can be also derived by imposing the stationarity of the energy functional $E(\bar{\mathbf{c}}) = \langle \phi | \mathcal{H}_0 | \phi \rangle / \langle \phi | \phi \rangle$.